Pedestrian dynamic response and injury risk in high speed vehicle crashes

JIN NIE[1], XIAOJIANG LV[2], XING HUANG[3]*, KUI LI[4], GUIBING LI[5]

[1] Loudi Vocational and Technical College, Loudi, China.
[2] Zhejiang Key Laboratory of Automobile Safety Technology, Geely Automobile Research Institute, Ningbo, China.
[3] Medical Imaging Center, The First People's Hospital of Chenzhou, Chenzhou, China.
[4] Chongqing Key Laboratory of Vehicle Crash/Bio-Impact and Traffic Safety, Institute for Traffic Medicine,
Daping Hospital, Army Medical University, Chongqing, China.
[5] School of Mechanical Engineering, Hunan University of Science and Technology, Xiangtan, China.

Purpose: The purpose of the current study is to understand pedestrian kinematics, biomechanical response and injury risk in high speed vehicle crashes. *Methods:* Vehicle-to-pedestrian crashes at the impact speeds of 40 km/h (reference set) and 70 km/h (analysis set) were simulated employing FE models of a sedan front and an SUV front together with a pedestrian FE model developed using hollow structures. The predictions from crash simulations of different vehicle types and impact speeds were compared and analyzed. *Results*: In crashes at 70 km/h, pedestrian head-vehicle contact velocity is by about 20–30% higher than the vehicle impact speed, the peak head angular velocity exceeds 100 rad/s and is close to the instant of head-vehicle contact, brain strain appears two peaks and the second peak (after head contact) is obviously higher than the first (before head contact), and AIS4+ head injury risk is above 50%, excessive thorax compression induces rib fractures and lung compression, both sedan and SUV cases show a high risk (>70%) of AIS3 + thorax injury, and the risk of AIS4 + thorax injury is lower than 40% in the sedan case and higher than 50% for the SUV case. *Conclusions*: Pedestrians in vehicle crashes at 70 km/h have a higher AIS3 + /AIS4 + head and thorax injury risk, high vehicle impact speed is more easily to induce a high head angular velocity at the instant of head-vehicle contact, brain strain is strongly associated with the combined effect of head rotational velocity and acceleration, and pedestrian thorax injury risk is more sensitive to vehicle impact speed than the head.

Key words: pedestrian kinematics, pedestrian biomechanical response, injury risk, high speed vehicle crash

1. Introduction

Studies have proved that the New Car Assessment Programs (NCAP) have improved vehicle safety performance for pedestrian protection by employing the subsystem impact tests [12], [13], [17], [24]. However, almost all NCAPs in the world only focus on the vehicle impact speeds at or below 40 km/h [1], [2], which can only cover the pedestrian cases below 5% fatality risk, i.e., more than 95% of pedestrian deaths occurred in the vehicle impacts above 40 km/h [19], [22]. The current situation is that more than 270,000 pedestrians are still killed on the road every year [29].

These may suggest that current vehicle passive safety evaluation for pedestrian protection should raise the requirements to focus on the scenarios at an impact speed significantly higher than 40 km/h, where kinematical and biomechanical understanding on pedestrian response in crashes at high impact speeds are needed.

Currently, finite element (FE) modeling using human body models with high biofidelity has become the main approach for pedestrian safety research. In the past decades, FE simulations have provided a lot of valuable information for understanding of pedestrian injury mechanism and vehicle front-end safety design. For example, isolated body lower limb models

were employed in analysis of pedestrian leg injury mechanism and vehicle bumper system optimization [9], [15], [16], [23]; the THUMS (Total Human Model for Safety) model was widely used for studies of pedestrian kinematics and injury prediction [5], [10], [11], [20], [28]. However, most existing studies of pedestrian passive safety only considered the scenarios at the impact speeds of 40 km/h or below, kinematical and biomechanical understanding on pedestrian response in crashes at a high impact speed is scare. On the other hand, vehicle-to-pedestrian crash simulations at high impact speeds are limited due to the poor computational stability of human body FE models, as most human body FE models were developed using solid elements which are easy to cause error termination of simulations from negative volume in high speed impacts. To solve this issue, the authors of the current study recently developed and validated a pedestrian FE model with high computational stability in high impact energy scenarios [10], which can be used as the effective tool for pedestrian biomechanical analysis in high speed vehicle crashes.

Therefore, the purpose of the current study is to analyze pedestrian kinematics, biomechanical response and injury risk in high speed vehicle crashes using FE simulations. To achieve this, the recently developed pedestrian FE model with high computational stability were employed, and comparative analysis was conducted between vehicle crashes at high (70 km/h) and mid-high (40 km/h, as the reference) speeds, and between sedan and SUV impacts. Since most serious and fatal injuries are to the head and thorax, the analysis mainly focuses on the response of pedestrian head and thorax.

2. Materials and methods

2.1. The pedestrian FE model with hollow structures

In a previous study [10], Li et al. developed a pedestrian FE model with high computational efficiency and stability by replacing the subcutaneous fat and skeletal muscle in the THUMS model with hollow structures (HS), named as THUMS-HS pedestrian model (Fig. 1). In the THUMS-HS pedestrian model all tissues of the head, ribcage and internal organs were kept as defined in the original THUMS mode (i.e., solid elements); the fat and skeletal muscle were modeled as hollow structures with grids in the size of 30 × 30 ×

30 mm using shell elements of 1.5 mm in thickness and plastic material which can predict the mechanical properties of the solid skeletal muscle and subcutaneous fat [10]. The biofidelity of the THUMS-HS pedestrian model was validated against cadaver tests data and showed good match to the test results [10], particularly the predicted mechanical properties such as force-displacement and moment-displacement curves from the lower limb, force time history curves from the pelvis, abdomen, thorax and shoulder were within the corridors of cadaver test data. Additionally, the trajectories of the head, T1, T8 and pelvis of the THUMS-HS model in a sedan impact were close to those of the average level of cadaver tests [10]. The THUMS-HS pedestrian model also showed high computational efficiency, and stability in vehicle-to-pedestrian crash simulations [10]. Considering the good properties of high biofidelity and high computational efficiency, and stability, the THUMS-HS pedestrian model was employed to predicate pedestrian kinematics and biomechanical response in vehicle crashes in the current work. In the current work, strain thresholds was defined to leg long bones (tibia = 0.015, fibula = 0.023 and femur = 0.017) and ribs (0.025) in the THUMS-HS model for simulating fractures, while skull fracture was not considered since the deleted meshes in realizing fractures by FE method may distort the brain response.
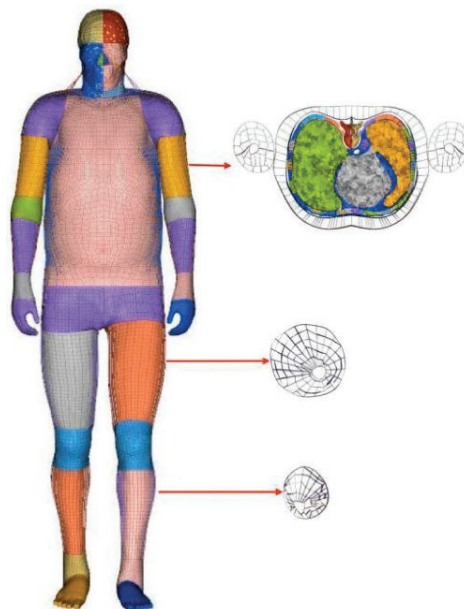

Fig. 1. The THUMS-HS pedestrian model

2.2. Vehicle front FE models

To consider the common vehicle types on the road, FE models of a sedan (Toyota Camry 2012) front and
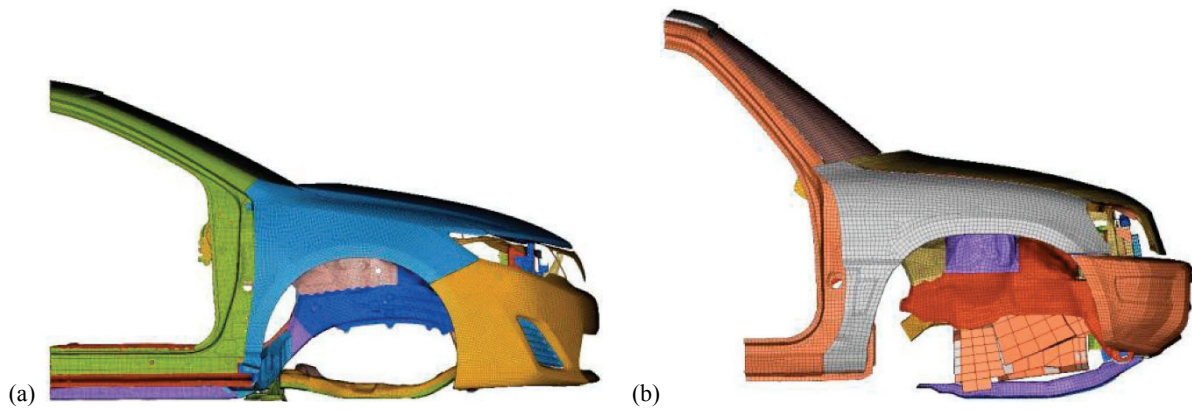
Fig. 2. Vehicle front FE models of sedan (a) and SUV (b)

an SUV (Toyota RAV4 1997) front were created based on the full scale vehicle models downloaded from the NCAC website [17]. The frontal structures of the original vehicle models were extracted with the rear part of both vehicle models being removed from the A-pillar, where the mass of the removed parts (behind A-pillar) was attached to the vehicle front parts to keep the total mass of the full vehicle, and the position of the attached mass was set to keep the location of center of mass (Fig. 2). The material properties of the windshield were redefined using the parameters evaluated using pedestrian head impactor tests in a previous study [21].

2.3. Vehicle-to-pedestrian crash modeling

Based on the above mentioned THUMS-HS pedestrian model and vehicle front FE models, vehicle-to-pedestrian crash simulation models were developed (Fig. 3). For a comparative analysis, vehicle-to-pedestrian crash simulations were defined at the speed of 40 km/h (reference set) and 70 km/h (analysis set),

respectively. The impact speed (40 km/h) for the reference set was based on the impact speed in C-NCAP and Euro-NCAP subsystem tests [1], [2], while the 70 km/h selected for the analysis set was according to the 50% pedestrian fatality risk observed from real world accidents [19], [22]. Similarly to previous studies [5], [11], [20], the initial contact location was set at the center line of the vehicle in the width direction and friction coefficients of 0.3 and 0.7 were applied to the pedestrian-vehicle contact and pedestrian-ground contact respectively. The above-mentioned vehicle-to-pedestrian crashes were calculated under the environment of LS-DYNA software [14].

The predicted dynamic response including overall kinematics, brain strain distribution and thorax compression from the simulations were employed for analysis. Head injury criterion CSDM (Cumulative Strain Damage Measure) and thorax criterion injury NHTD (Normalized Half Thorax Deflection) were then calculated from the predicted brain strain and thorax compression, respectively. These selected injury criteria can reflect biomechanical response of the corresponding body regions and were wildly used for assessing serious injuries together with the risk curves for AIS4+
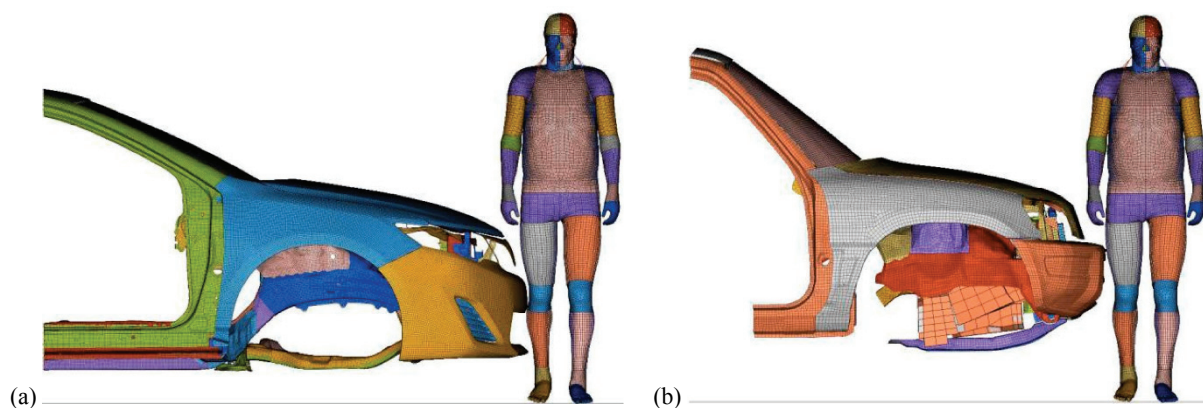

Fig. 3. Vehicle-to-pedestrian impact simulation setup: sedan crash (a) and SUV crash (b)

injuries [7], [11], [25]–[27]. To show the difference, the predictions from the simulations at 70 km/h were compared with those from crashes at 40 km/h.

3. Results

3.1. Pedestrian kinematics

In Figure 4, the predicted overall kinematics of the THUMS-HS pedestrian model in sedan and SUV crashes at the impact speed of 70 km/h and 40 km/h, respectively, are shown. For sedan crashes, when the impact speed is 70 km/h, the upper body tends to rotate at about 30 ms with the thorax thorax-bonnet (rear part) contact at 60 ms and head-windscreen (middle-lower part) contact at 80 ms, while in the 40 km/h impact, the upper body tends to rotate at about 40 ms, the thorax-bonnet (central part) contact and head-bonnet (rear end) contact occur at 80 ms and 115 ms, respectively. For the SUV crash at 70 km/h, thorax-bonnet (rear part) contact starts from about 45 ms and head-windscreen (lower edge) contact time is at 70 ms; while in the SUV crash at 40 km/h, the thorax-bonnet
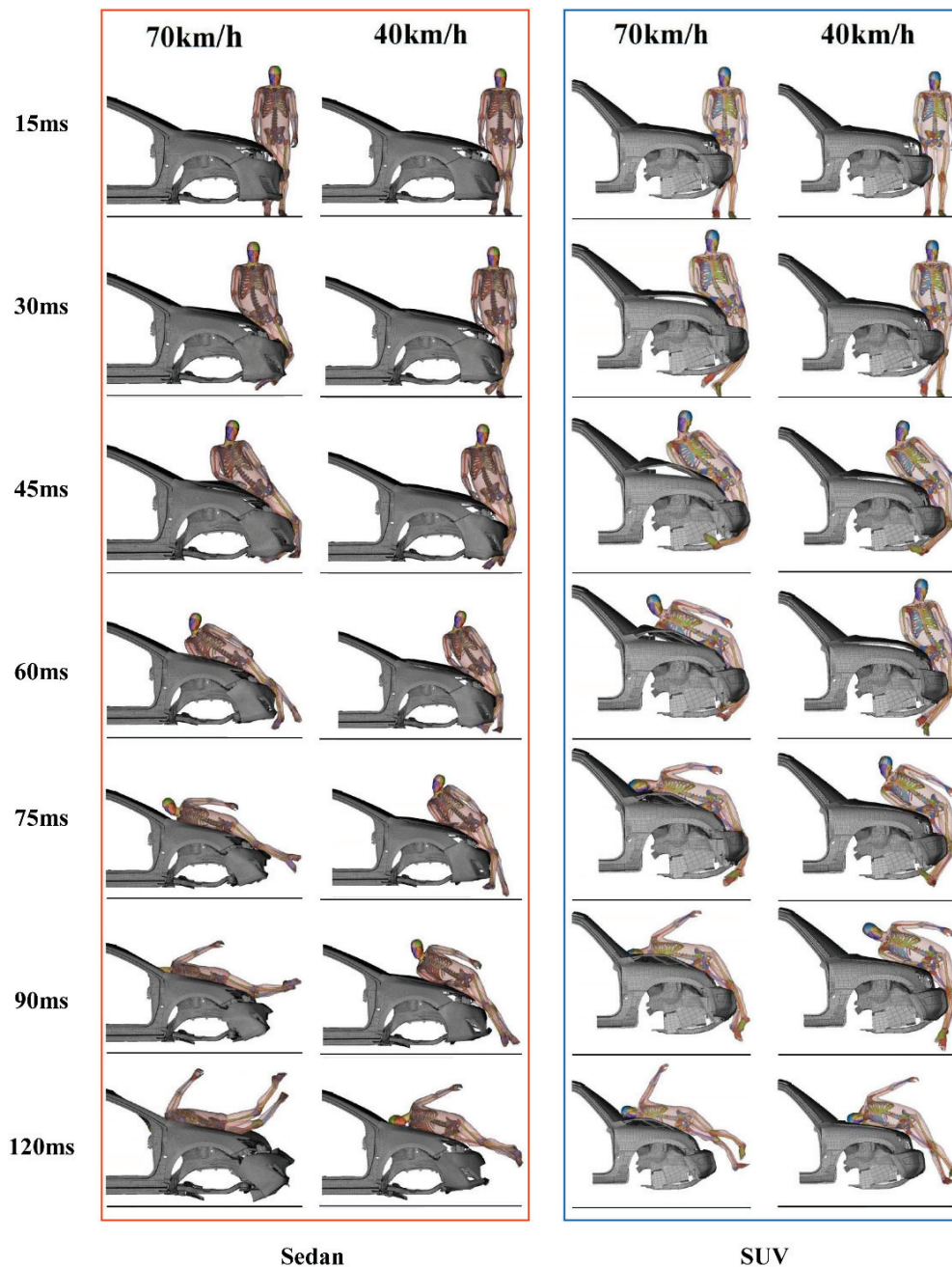

Fig. 4. Pedestrian kinematics in sedan and SUV crashes at 70 km/h and 40 km/h
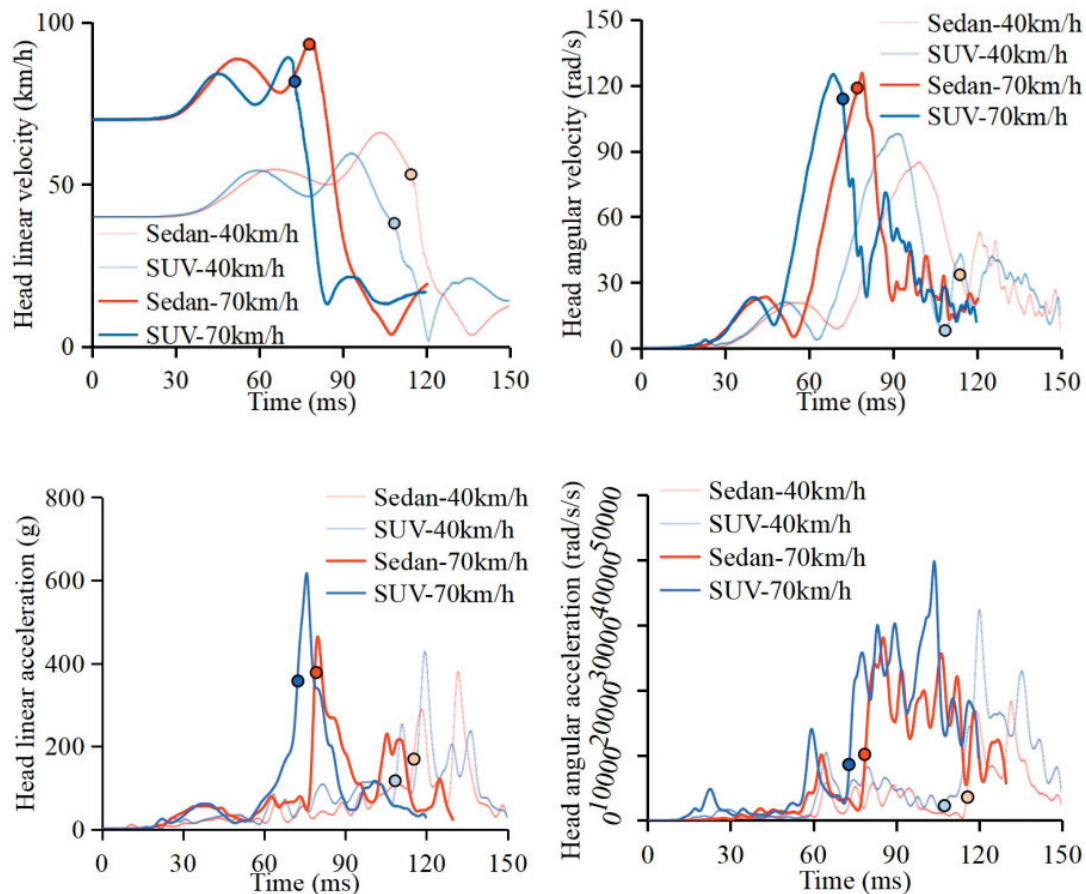
Fig. 5. Time history of pedestrian head linear velocity (related to the vehicle), angular velocity, liner acceleration and angular acceleration in sedan and SUV crashes (the dots on the curves indicate the head contact time)

(central part) contact and head-bonnet (rear end) contact happen at 65 ms and 110 ms, respectively. Clearly, there is more sliding of the pedestrian on the vehicle bonnet in the crashes at 70 km/h than those of 40 km/h for both sedan and SUV cases.

In Figure 5, pedestrian head contact velocity (linear and angular) and acceleration (linear and angular) predicted from crashes under different impact boundary conditions are compared. The general trends of head linear or angular velocity as a function of time are similar between different crashes, while the peak value, peak time, and contact velocity (the velocity at the instant of head contact) are distinguished. At the instant of head contact its linear velocity is 94 km/h and the angular velocity is 122 rad/s in sedan crashes at 70 km/h, these are significantly lower in crashes at 40 km/h (head linear velocity = 53 km/h and angular velocity = 29 rad/s). For the SUV case, the head linear contact velocity is 82 km/h with an angular velocity of 110 rad/s when the pedestrian was struck at 70 km/h, which are obviously higher than those (head linear velocity = 36 km/h, angular velocity = 13 rad/s) in the crash at 40 km/h. The maximum head linear

acceleration is 456 g and 608 g for sedan and SUV crash at 70 km/h receptively, and the peak time is about 5 ms after the head contact. The maximum head linear acceleration is 368 g and 421 g for sedan and SUV crash at 40 km/h, respectively, and which occur at the second peak in the time 10–15 ms after head contact. For head angular acceleration, in crashes at 70 km/h (vs. 40 km/h), the maximum value is about 40000 rad/s/s (vs. 31400 rad/s/s) in the SUV case and exceeds 27000 rad/s/s (vs. 19300 rad/s/s) in the sedan case, and a obviously larger peak width was observed in the impacts at 70 km/h.

3.2. Head and thorax biomechanical response

The predicted brain strain distribution and thorax compression in sedan and SUV crashes are shown in Figs. 6 and 7, respectively. The brain of the THUMS-HS model experienced two strain peaks during the crashes (Fig. 6). The deformation direction of the brain is opposite to each other between these two
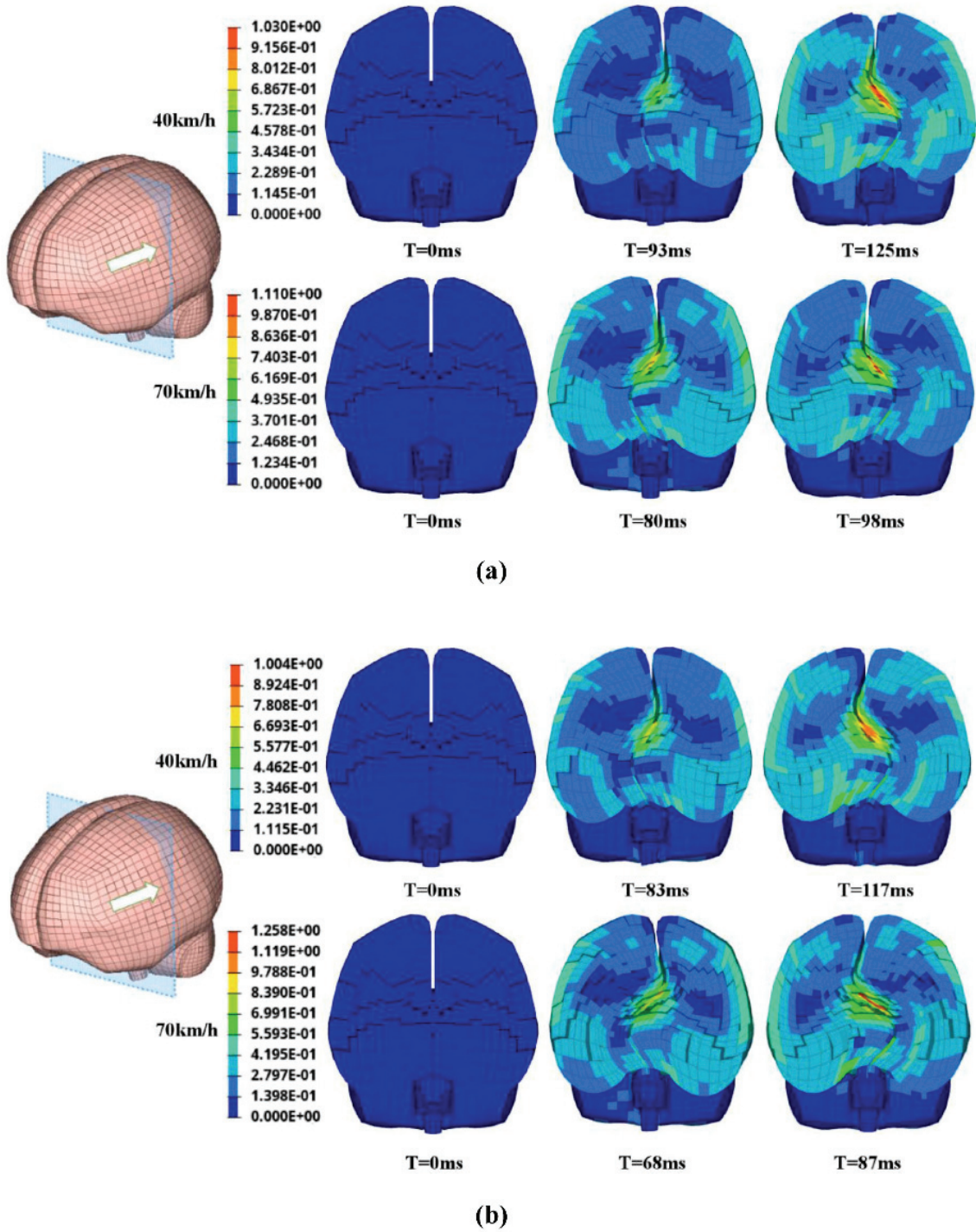
Fig. 6. Predicted brain strain distribution in sedan (a) and SUV (b) crashes

strain peaks, where the brain deforms toward the vehicle during the first strain peak, while this is toward the direction of vehicle moving at the second strain peak. The first brain strain peak is at the time near head contact in crashes at 70 km/h, but this occurs at the time about 20 ms before the head contact time in crashes at 40 km/h. The second brain strain peak appears at the time 10–20 ms after head contact for all crashes. Generally, the brain shows more serious strain in crashes at 70 km/h than 40 km/h. In Figure 7, obvious compression to the thorax of the THUMS-HS model in both sedan and SUV crashes at 70 km/h can be seen, which is more serious than that of crashes at 40 km/h. The excessive thorax compression in crashes at 70 km/h induces rib fractures and lung compression (Fig. 8).
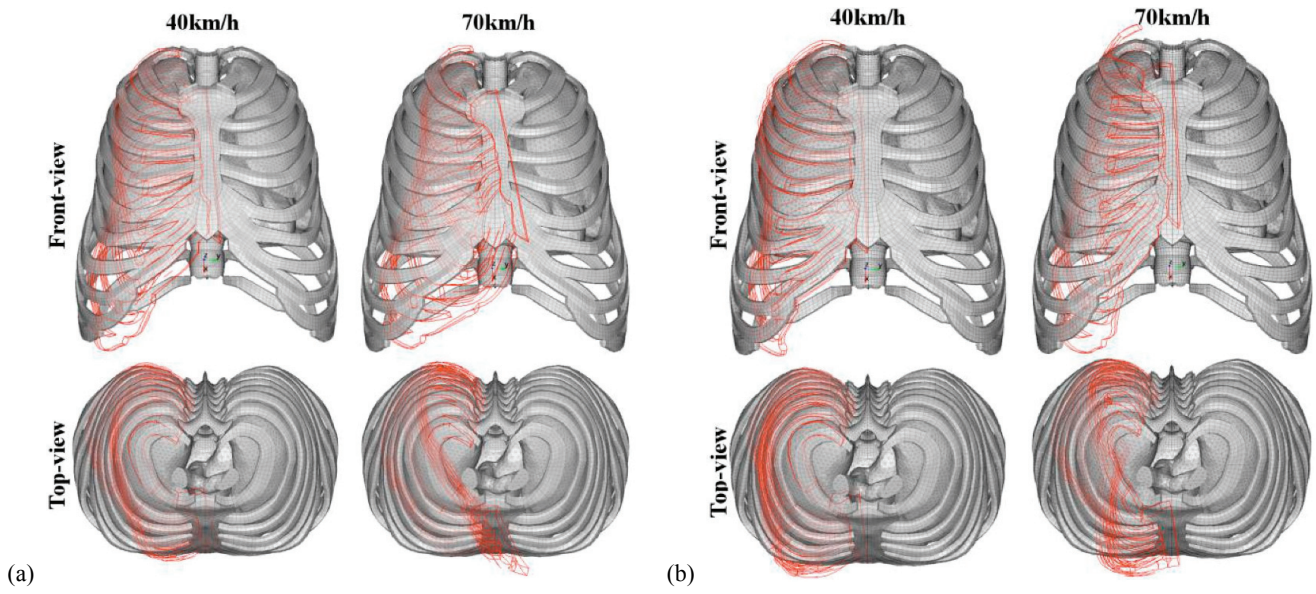
Fig. 7. Predicted thorax compression in sedan (a) and SUV (b) crashes
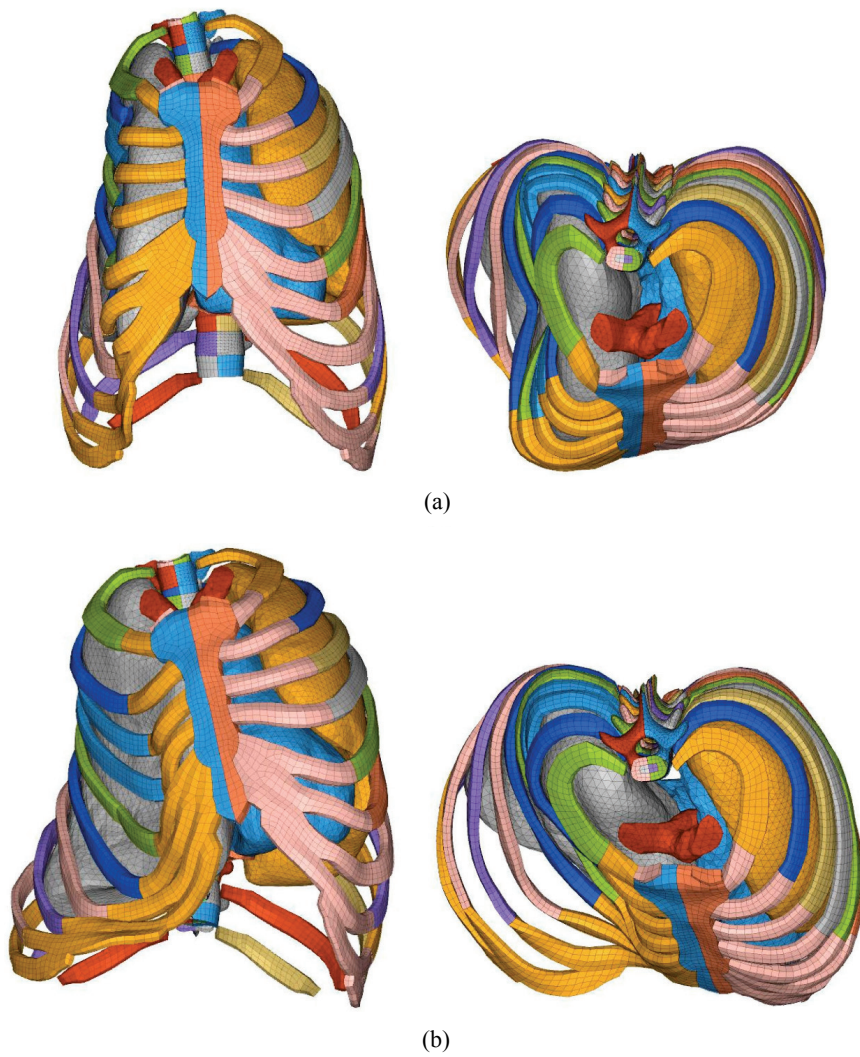(the ribcage in red shows the maximum deformation)

Fig. 8. Predicted rib fractures and lung compression in sedan (a) and SUV (b) crashes at 70 km/h (struck from the right side)

3.3. Head and thorax injury risk

In Figure 9, the probabilities of serious (AIS3+/AIS4+) head and thorax injuries estimated based on the predicted CSDM (the critical level of 0.25 was

protection should use an WAD higher than 2,100 mm if scenarios at high impact speeds are to be considered. Thankfully, the updated test procedures in Euro-NCAP and C-NCAP extended the headform impactor test area from WAD of 2,100 mm to 2,300 mm, but the impact speed is still at 40 km/h [1], [2].
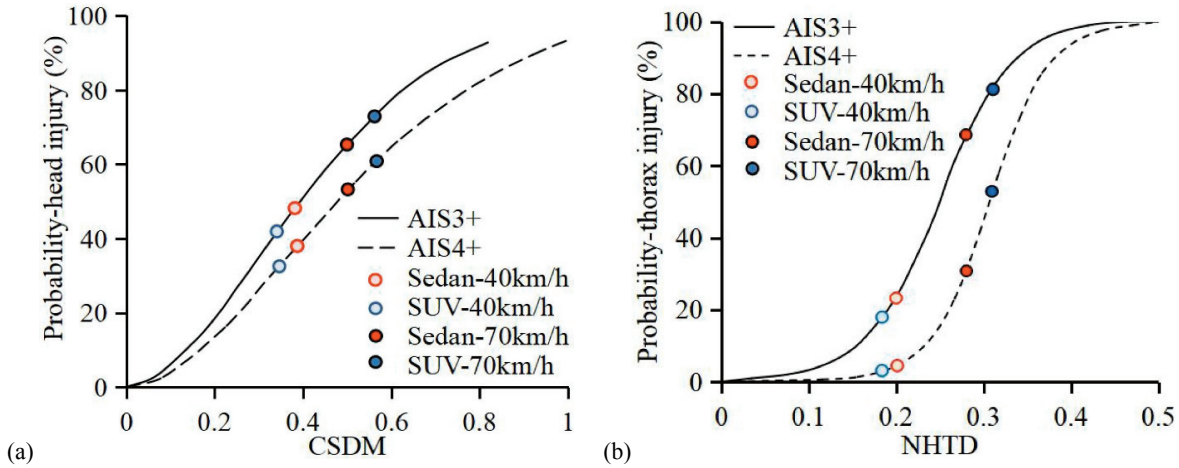

Fig. 9. Predicted head (a) and thorax (b) injury risk based on the predicted CSDM and NHTD

used) and NHTD values are shown. The injury risk curves for the head and thorax are from the study of Takhounts et al. [25] and Kuppa et al. [7], respectively. CSDM0.25 values indicate that the risk of AIS3+ head injury is above 60%, while AIS4+ head injury risk is above 50% for sedan and SUV crashes at 70 km/h, and this is below 40% in crashes at 40 km/h. For crashes at 70 km/h, both sedan and SUV cases show a high risk (>70%) of AIS3+ thorax injury, the risk of AIS4+ thorax injury is lower than 40% in the sedan case and higher than 50% for the SUV case. The predicted risks of AIS3+ and AIS4+ thorax injury are lower than 30% for crashes at 40 km/h.

4. Discussion

4.1. Kinematics

In Figure 4, it can be seen that the head contact location in the simulations at 70 km/h is on the windscreen area for both sedan and SUV crashes, the head WAD (measured wrap distance) is 2,120 mm and 2,080 mm for the sedan and SUV case, respectively. The head contact location for the crashes at 40 km/h is on the bonnet rear end area, where has a shorter WAD (sedan = 1910 mm, SUV = 1760 mm). This may suggest that the vehicle safety evaluation for pedestrian head

The predicted results indicate that the head contact time in crashes at 70 km/h is before 80 ms (Figs. 4, 5), which is much earlier than that (after 100 ms) of the collisions at 40 km/h. This implies that development of pedestrian airbags needs to consider the variation of head contact time from vehicle impact speed. The head linear velocity at the instant of head-to-vehicle contact in crashes at 70 km/h is clearly (by about 20–30%) higher than the vehicle initial speed, and this trend is more significant in the sedan case (head linear contact velocity = 94 km/h) than the SUV case (head linear contact velocity = 82 km/h) (Fig. 5). In crashes at 40 km/h, the head linear contact velocity is higher than the vehicle speed in the sedan case (head linear contact velocity = 53 km/h), but lower than the vehicle impact speed in the SUV case (head linear contact velocity = 36 km/h) (Fig. 5). The head angular velocity at the instant of head-to-vehicle contact in crashes at 70 km/h exceeds 100 rad/s and the peak of head angular velocity is close to the head contact time (Fig. 5). By contrast, in the crashes at 40 km/h, the head angular velocity at the instant of contact is below 30 rad/s and the peak head angular velocity appears about 15 ms before the head contact (Fig. 5). This indicates that the high vehicle impact speed is more easily to induce a high head rotation velocity at the instant of head-vehicle contact. A previous study reported that head rotation velocity above 50 rad/s together with linear contact velocity above 30 km/h could substantially

increase pedestrian head injury risk in vehicle crashes. This may suggest that greater attention should be paid to head rotation motion in high speed vehicle crashes than collisions at middle-lower speed. The sedan cases show a higher head rotation than SUV cases for all simulations. It seems that the relatively lower ratio of bonnet leading edge height to that of human body center of gravity in the sedan case raises the rotation of the upper body, hence, increasing head impact velocity. Similar trend was also observed in previous studies [5], [6]. The above findings indicate big differences in head kinematics between crashes at 70 km/h and 40 km/h and may provide reference for headform impactor tests considering pedestrian head protection in high speed vehicle crashes.

4.2. Biomechanical response

The biomechanical response indicates that high strain is mainly to the central and marginal regions of the brain tissue (Fig. 6). This is due to the fact that the translational and rotational motion of the head result in deformation and shear to the brain entity and brain-skull interface, where greater inertia in the central region causes high strain, and the marginal region is stretched by shear force inducing high strain. The brain strain appears two peaks and the second peak (after head contact) is obviously higher than the first (before head contact) (Fig. 6). This is because that the first peak occurs before head-vehicle contact due to head rotation without linear impact, while the second peak (after head contact) was caused by combined load of head linear impact and rotation, which is stronger than the load of rotation only. The results also show that the vehicle impact speed only affects the magnitude of pedestrian brain strain but not the general trend. Combining the results presented in Figs. 5 and 6, it can be found that the first brain strain peak occurs at the time close to the maximum value of head rotation velocity, and the angular acceleration peak (occurring at the time of the second brain strain peak) aggravates the brain strain together with the angular velocity, though, the angular velocity at the time of second brain strain peak is lower than that at the time of first brain strain peak. These findings suggest that brain strain is strongly associated with the combined effect of head rotational velocity and acceleration, which is inline with previous view on mechanisms for brain injuries [3], [4], [27]. The above findings suggest that reducing vehicle impact speed, stiffness of head contacting area and pedestrian head rotation motion would benefit for pedestrian protection.

Simulation results show severe ribcage compression to the pedestrian in vehicle crashes at 70 km/h, which lead to multi rib fractures and large lung compression and hence high injury risk (Figs. 8 and 9). While the compression of pedestrian ribcage is relatively small in vehicle crashes at 40 km/h, the predicted thorax injury risk is also low (Figs. 7 and 9). These implies that pedestrian thorax compression is highly sensitive to vehicle impact speed. This is because that pedestrian thorax compression is from blunt impact load from contact with the bonnet, where the impact energy is mainly determined by the contact velocity which strongly associated with vehicle impact speed. Considering compression and its rate (or velocity) are both key factors for mechanism of human thorax injury [8], [26], the situation in high vehicle impact speed is much worse. On the other hand, the difference in pedestrian thorax compression between sedan and SUV crash at 70 km/h is bigger than that in crashes at 40 km/h, since the high impact energy in crashes at 70 km/h leads to large bonnet deformation to reach the underlying stiff points. Thus crashes at high impact speeds require much larger bonnet deformation space.

4.3. Injury risk

The predictions show that the pedestrian head has a high risk of AIS4 + injury and thorax has a high risk of AIS3 + injury in crashes at 70 km/h, which are significantly higher than those in the cases at 40 km/h (Fig. 9). The high linear (>80 km/h) and angular (>100 rad/s) head impact velocity together resulted the high AIS4+ head injury risk in crashes at 70 km/h. The predicted AIS4 + head injury risk is higher in SUV crash than that of sedan case at 70 km/h (Fig. 9), though the head has a higher linear and angular velocity at the instant of head-to-vehicle contact in the sedan case (Fig. 5). This might be mainly due to the higher stiffness of head contact location in the SUV crash, where the head contact location is closer to the windscreen lower frame (Fig. 4). The area close to the windscreen lower frame still threaten pedestrian head safety as reported in NCAP tests even at 40 km/h. There is no doubt that contacts on this area leaded to high head injury risk in as observed in current simulations when the impact speed is much higher than 40 km/h. For the thorax, the simulations indicate that the risk for AIS3+/AIS4+ thorax injury in vehicle crashes at 40 km/h is low (<30%), but the gap in pedestrian thorax injury risk between crashes at 70 km/h and 40 km/h is much greater than that for head injury

(Fig. 9). This may imply that pedestrian thorax injury risk is more sensitive to vehicle impact speed than the head. There are two reasons for this finding, one is that the head injury risk to brain strain is not as sensitive as the thorax injury risk to its compression, another is that the brain strain is not as sensitive to vehicle impact speed as thorax compression.

The above findings suggest that the current vehicle are still faraway from safe design for pedestrian head and thorax protection in high speed crashes, though most vehicle models showed good performance in headform impactor tests (impact speed = 40 km/h) as reported by C-NCAP (https://www.c-ncap.org/) and Euro-NCAP (https://www.euroncap.com/). Given the difficult in improving vehicle design, pre-crash speed control based on active safety system such as AEB might be the effective way to reduce pedestrian serious and fatal injury risk on the road.

4.4. Limitations

There are several limitations to the current study. Firstly, only one high impact speed and two vehicle models were selected for analysis though there are both representative, more crash scenarios would be considered in further work. Secondly, the THUMS-HS pedestrian model has been validated for predicting cadaver kinematics and mechanical response, but the detailed tissue response has not been validated in actual pedestrian impact cases. However, considering the good predicative capability of the original THUMS model in reconstruction of pedestrian thorax and head injuries [11], and the consistency of the the THUMS-HS model and THUMS model in bone and internal organs [10], the predictions in the current study are plausible. The suspension characteristics was not considered in the simplified vehicle front model since this is supposed to be not sensitive to pedestrian response. Nonetheless, the analysis has shown new insights into pedestrian kinematics and biomechanical response in vehicle crash loading and these predictions can be used to guide future vehicle safety assessment and design.

5. Conclusions

The current study makes the first attempt to understand pedestrian kinematics and biomechanical response in high speed vehicle crashes. The modeling results indicate significant differences in pedestrian overall kinematics and head and thorax biomechanical re-

sponse between vehicle crashes at 70 km/h and 40 km/h. In particular, compared to crashes at 40 km/h pedestrians in vehicle crashes at 70 km/h have a earlier head and thorax contact time and longer WAD, high head contact velocity, more serious brain rotation and higher brain strain, bigger thorax compression, and hence a higher AIS3+/AIS4+ head and thorax injury risk. The analysis indicates that high vehicle impact speed is more easily to induce a high head angular velocity at the instant of head-vehicle contact, brain strain is strongly associated with the combined effect of head rotational velocity and acceleration, and pedestrian thorax injury risk is more sensitive to vehicle impact speed than the head. The observed high risk of serious head and thorax injuries to pedestrians in high speed vehicle crashes imply that it is still a big gap to achieve safe vehicle design for pedestrian protection in all accident scenarios.

Acknowledgements

References

[1] C-NCAP. C-NCAP Management Regulation (2021 Version). China New Car Assessment Programme. China Automotive Technology and Research Center, 2020.

[2] Euro-NCAP. Assessment Protocol-Vulnerable Road User Protection, Version 10.0.3. European New Car Assessment Programme, 2020.

[3] GENNARELLI T., OMMAYA A., THIBAULT L., *Comparison of translational and rotational head motions in experimental cerebral concussion*, SAE Technical Paper, No. 710882, 1971.

[4] GENNARELLI T., THIBAULT L., OMMAYA A., *Pathophysiologic responses to rotational and translational accelerations of the head*, SAE Technical Paper, No. 720970, 1972.

[5] HAN Y., YANG J., NISHIMOTO K., MIZUNO K., MATSUI Y., NAKANE D., WANAMI S., HITOSUGI M., *Finite element analysis of kinematic behaviour and injuries to pedestrians in vehicle collisions*, Int. J. Crashworthiness, 2012, 17 (2), 141–152.

[6] KERRIGAN J., CRANDALL J., DENG B., *A comparative analysis of the pedestrian injury risk predicted by mechanical impactors and post mortem human surrogates*, Stapp Car Crash J., 2008, 52 (1), 527–567.

[7] KUPPA S., EPPINGER R., MCKOY F., NGUYEN T., PINTAR F., YOGANANDAN N., *Development of side impact thoracic injury criteria and their application to the modified ES-2 dummy with rib extensions (ES-2re)*, Stapp Car Crash J., 2003, 47, 189–210.

[8] LAU I., VIANO D., *The viscous criterion-bases and applications of an injury severity index for soft tissues*, SAE Technical Paper, No. 861882, 1986.

[9] LI G., MA H., GUAN T., GAO G., *Predicting safer vehicle front-end shapes for pedestrian lower limb protection via a numerical optimization framework*, Int. J. Auto. Tech.-Kor., 2020, 21 (3), 749–756.

[10] LI G., MENG H., LIU J., ZOU D., LI K., *A novel modeling approach for finite element human body models with high computational efficiency and stability: application in pedestrian safety analysis*, Acta Bioeng. Biomech., 2021, 21 (2), 21–30.

[11] LI G., TAN Z., LV X., REN L., *Numerical reconstruction of injuries in a real world minivan-to-pedestrian collision*, Acta Bioeng. Biomech., 2019, 21 (2), 21–30.

[12] LI G., WANG F., OTTE D., CAI Z., SIMMS C., *Have pedestrian subsystem tests improved passenger car front shape?*, Accid. Anal. Prev., 2018, 115, 143–150.

[13] LI G., WANG F., OTTE D., SIMMS C., *Characteristics of pedestrian head injuries observed from real world collision data*, Accid. Anal. Prev., 2019, 129, 362–366.

[14] LSTC. LS-DYNA keyword user's manual, version 971. Livermore Software Technology Corporation Livermore, United States of America, 2007.

[15] MO F., LUO D., TAN Z., SHANG B., ZHOU D., *A human active lower limb model for Chinese pedestrian safety evaluation*, J. Bionic. Eng., 2021, 18 (4), 872–886.

[16] MO F., ARNOUX P.J., CESARI D., MASSON C., *Investigation of the injury threshold of knee ligaments by the parametric study of car-pedestrian impact conditions*, Saf. Sci., 2014, 62, 58–67.

[17] NCAC. National Crash Analysis Center Vehicle Model Library, http://www.ncac.gwu.edu/vml/models.html, 2014 [accessed: 16 September 2014].

[18] NIE B., ZHOU Q., *Can new passenger cars reduce pedestrian lower extremity injury? A review of geometrical changes of front-end design before and after regulatory efforts*, Traffic Inj. Prev., 2016, 17 (7), 712–719.

[19] NIE J., LI G., YANG J., *A study of fatality risk and head dynamic response of cyclist and pedestrian based on passenger car accident data analysis and simulations*, Traffic Inj. Prev., 2015, 16 (1), 76–83.

[20] PAAS R., DAVIDSSON J., BROLIN K., *Head kinematics and shoulder biomechanics in shoulder impacts similar to pedestrian crashes-a THUMS study*, Traffic Inj. Prev., 2015, 16, 498–506.

[21] PENG Y., YANG J., DECK C., WILLINGER R., *Finite element modeling of crash test behavior for windshield laminated glass*, Int. J. Impact Eng., 2013, 57 (7), 27–35.

[22] ROSÉN E., SANDER U., *Pedestrian fatality risk as a function of car impact speed*, Accid Anal. Prev., 2009, 41 (3), 536–542.

[23] SCATTINA A., MO F., MASSON C., AVALLE M., ARNOUX P., *Analysis of the influence of passenger vehicles front-end design on pedestrian lower extremity injuries by means of the LLMS model*, Traffic Inj. Prev., 2018, 19 (5), 535–541.

[24] STRANDROTH J., STERNLUND S., LIE A., TINGVALL C., RIZZI M., KULLGREN A., OHLIN M., FREDRIKSSON R., *Correlation between Euro-NCAP pedestrian test results and injury severity in injury crashes with pedestrians and bicyclists in Sweden*, Stapp Car Crash J., 2014, 58, 213–231.

[25] TAKHOUNTS E., CRAIG M., MOORHOUSE K., MCFADDEN J., HASIJA V., *Development of brain injury criteria (BrIC)*, Stapp Car Crash J., 2013, 57, 243–266.

[26] VIANO D., *Biomechanical responses and injuries in blunt lateral impact*, SAE Technical Paper No. 892432, 1989.

[27] WANG F., YU C., WANG B., LI G., MILLER K., WITTEK A., *Prediction of pedestrian brain injury due to vehicle impact using computational biomechanics models: Are head-only models sufficient?*, Traffic Inj. Prev., 2020, 21 (1), 102–107.

[28] WATANABE R., KATSUHARA T., MIYAZAKI H., KITAGAWA Y., YASUKI T., *Research of the relationship of pedestrian injury to collision speed, car-type, impact location and pedestrian sizes using human FE model (THUMS version 4)*, Stapp Car Crash J., 2012, 56, 269–321.

[29] WHO. Global status report on road safety 2018: Summary (No.WHO/NMH/NVI/18.20), World Health Organization, Geneva, Switzerland, 2018.